Chapter 1

Tau Decays into Hadrons

Building on the previously presented QCDSR we will elaborate the needed theory to extract α_s from the process of hadronic tau decays. ... complete

1.1 Tau Decays into hadrons

The tau lepton is the only lepton heavy enough to decay into hadrons. It permits one of the most precise determinations of the strong coupling α_s. The inclusive tau decay ratio

$$R_\tau = \frac{\Gamma(\tau \to \nu_\tau + \text{hadrons})}{\Gamma(\tau \to \nu_\tau e^+ e^-)} \tag{1.1.1}$$

can be precisely calculated and is sensitive to α_s. Due to the small mass of the tau lepton $m_\tau \approx 1.776\,\text{GeV}$ the tau decays are excellent for performing a low-energy QCD analysis. The theoretical expression of the hadronic tau decay ratio was first derived by [**Tsai1971**], using current algebra, a more recent derivation making use of the *optical theorem*, as already mentioned in **??** can be taken from [**Schwab2002**].

1.1.1 The Inclusive Decay Ratio

The inclusive ratio is given by:

$$R_\tau(s) = 12\pi S_{EW}|V_{ud}|^2 \int_0^{m_\tau} \frac{ds}{m_\tau^2}\left(1-\frac{s}{m_\tau^2}\right)\left[\left(1+2\frac{s}{m_\tau^2}\right)\text{Im}\,\Pi^{(1)}(s) + \text{Im}\,\Pi^{(0)}(s)\right], \tag{1.1.2}$$

where S_{EW} is the electro-weak correction, V_{ud} the corresponding *Cabibbo-Kobayashi-Maskawa* (CKM) matrix element and $\mathrm{Im}\,\Pi$ is imaginary part of the two-point function we introduced in **??**. For brevity we will omit the electro-weak S_{EW} and CKM factors from now on. redlongitudinal transversal decomposition. Applying Cauchy's theorem, as seen in **??**, to the eq. 1.1.2 we get

$$R_\tau = 6\pi i \oint_{s=m_\tau} \frac{ds}{m_\tau^2}\left(1-\frac{s}{m_\tau^2}\right)\left[\left(1+2\frac{s}{m_\tau^2}\right)\Pi^{(1)}(s)+\Pi^{(0)}(s)\right]. \tag{1.1.3}$$

It is furthermore convenient to work with $\Pi^{(T+L)}$, which has been defined in **??**. As a result we can further rewrite the hadronic tau decay ratio into

$$R_\tau = 6\pi i \oint_{|s|=m_\tau} \frac{ds}{m_\tau^2}\left(1-\frac{s}{m_\tau^2}\right)^2\left[\left(1+2\frac{s}{m_\tau^2}\right)\Pi^{(1+0)}(s)-\left(\frac{2s}{m_\tau^2}\right)\Pi^{(0)}(s)\right]. \tag{1.1.4}$$

In the case of tau decays we only have to consider vector and axial-vector contributions of decays into up, down and strange quarks. Thus taking i,j as the flavour indices for the light quarks (u, d and s) we can express the two-point function as

$$\Pi^{V/A}_{\mu\nu,ij}(s) \equiv i\int dx\, e^{ipx}\langle\Omega|T\{J^{V/A}_{\mu,ij}(x)J^{V/A}_{\nu,ij}(0)^\dagger\}|\Omega\rangle, \tag{1.1.5}$$

with $|\Omega\rangle$ being the physical vacuum. The vector and axial-vector currents are then distinguished by the corresponding dirac-matrices ($\gamma_\mu$and$\gamma_\mu\gamma_5$) given by

$$J^V_{\mu,ij}(x) = \overline{q}_j(x)\gamma_\mu q_i(x) \quad \text{and} \quad J^A_{\mu,ij}(x) = \overline{q}_j(x)\gamma_\mu\gamma_5 q_i(x). \tag{1.1.6}$$

With eq. 1.1.4 we have a suitable physical quantity that can be theoretically as experimentally obtained. As the circle contour integral we used is has a radius of s_0 we successfully avoided low energies at which the application of PT would be questionable. For example if we would choose a radius with the size of the tau mass $m_\tau \approx 1.78\,MeV$ the strong coupling would have a perturbatively safe value of $\alpha_s(m_\tau) \approx 0.33$ [**Pich2016**]. Obviously we would benefit even more from a contour integral over a bigger circumference, but tau decays are limited by their mass. Nevertheless there are promising e^+e^- annihilation data, which yields valuable R-ratio values up to $2\,GeV$ [**Boito2018**][**Keshavarzi2018**].

1.1.2 Renormalisation Group Invariance

We have seen in **??**, that the two-point function is not a physical quantity. From the dispersion relation (**??**) we saw that it contains a unphysical poly-

nom. Luckily for the vector correlator we are using in hadronic tau decays the polynom is just a constant. Consequently by taking the derivative with respect to the momentum s we can derive a physical quantity from the two-point function:

$$D(s) \equiv -s\frac{d}{ds}\Pi(s). \tag{1.1.7}$$

$D(s)$ is called the *Adler function* and fulfils the RGE (**??**). The Adler function commonly has separte definitions for the longitudinal plus transversal and the solely longitudinal part contributions:

$$D^{(1+0)}(s) \equiv -s\frac{d}{ds}\Pi^{(1+0)}(s), \qquad D^{(0)}(s) \equiv \frac{s}{m_\tau^2}\frac{d}{ds}(s\Pi^{(0)}(s)). \tag{1.1.8}$$

The two-point functions in **??** can now be replaced with the help of partial integration

$$\int_a^b u(x)v(x)\,dx = \left[U(x)V(x)\right]_a^b - \int_a^b U(x)v(x)\,dx. \tag{1.1.9}$$

We will do the computation for each of the two cases $(T+L)$ and (L) separate. Starting by the transversal plus longitudinal contribution we get:

$$\begin{aligned} R_\tau^{(1)} &= \frac{6\pi i}{m_\tau^2}\oint_{|s|=m_\tau^2} \underbrace{\left(1-\frac{s}{m_\tau^2}\right)^2\left(1+2\frac{s}{m_\tau^2}\right)}_{=u(x)}\underbrace{\Pi^{(1+0)}(s)}_{=V(x)} \\ &= \frac{6\pi i}{m_\tau^2}\left\{\left[-\frac{m_\tau^2}{2}\left(1-\frac{s}{m_\tau^2}\right)^3\left(1+\frac{s}{m_\tau^2}\right)\Pi^{(1+0)}(s)\right]_{|s|=m_\tau^2}\right. \\ &\quad \left.+\oint_{|s|=m_\tau^2}\underbrace{-\frac{m_\tau^2}{2}\left(1-\frac{s}{m_\tau^2}\right)^3\left(1+\frac{s}{m_\tau^2}\right)}_{=U(x)}\underbrace{\frac{d}{ds}\Pi^{(1+0)}(s)}_{=v(x)}\right\} \\ &= -3\pi i\oint_{|s|=m_\tau^2 s}\frac{ds}{s}\left(1-\frac{s}{m_\tau^2}\right)^3\left(1+\frac{s}{m_\tau^2}\right)\frac{d}{ds}D^{(1+0)}(s) \end{aligned} \tag{1.1.10}$$

where we fixed the integration constant to $C = -\frac{m_\tau^2}{2}$ in the second line and left the antiderivatives contained in the squared brackets untouched. If we parameterizing the integral appearing in the expression in the squared brackets we can see that it vanishes:

$$\left[-\frac{m_\tau^2}{2}\left(1-e^{-i\phi}\right)^3\left(1+e^{-i\phi}\right)\Pi^{(L+T)}(m_\tau^2 e^{-i\phi})\right]_0^{2\pi} = 0 \tag{1.1.11}$$

where $s \to m_\tau^2 e^{-i\phi}$ and $(1-e^{-i\cdot 0}) = (1-e^{-i\cdot 2\pi}) = 0$. Repeating the same calculation for the longitudinal part yields

$$\begin{aligned} R_\tau^{(0)} &= \oint_{|s|=m_\tau^2} ds \left(1-\frac{s}{m_\tau^2}\right)^2 \left(-\frac{2s}{m_\tau^2}\right) \Pi^{(0)}(s) \\ &= -4\pi i \oint \frac{ds}{s} \left(1-\frac{s}{m_\tau^2}\right)^3 D^{(0)}(s) \end{aligned} \tag{1.1.12}$$

Consequently combining the two parts results in

$$R_\tau = -\pi i \oint_{|s|=m_\tau^2} \frac{ds}{s} \left(1-\frac{s}{m_\tau^2}\right)^3 \left[3\left(1+\frac{s}{m_\tau^2} D^{(1+0)}(s) + 4D^{(0)}(s)\right)\right]. \tag{1.1.13}$$

It is convenient to define $x = s/m_\tau^2$ such that we can rewrite the inclusive ratio as

$$R_\tau = -\pi i \oint_{|s|=m_\tau^2} \frac{dx}{x}(1-x)^3 \left[3(1+x)D^{(1+0)}(m_\tau^2 x) + 4D^{(0)}(m_\tau^2 x)\right], \tag{1.1.14}$$

which will be the final expression we will be using to express the inclusive tau decay ratio.

1.2 Theoretical computation of R_τ

The previously derived expression for the tau decay ratio is at a first approximation equal to the number of colours

$$R_\tau \approx N_c. \tag{1.2.1}$$

If we take into account the CKM matrix V_{ud} and the perturbative δ_{pt}, non-perturbative δ_{npt} and electroweak corrections S_{EW} we can organise the vector and axial-vector inclusive decay ratio as

$$R_{\tau,V/A}^{\omega} = \frac{N_c}{2} S_{EW} |V_{ud}|^2 \left(1 + \delta_{pt}^{\omega} + \delta_{npt}^{\omega}\right). \tag{1.2.2}$$

Note that the factor $1/2$ comes from the fact that in the chiral limit the vector and axial-vector contributions are equal and that the perturbative and non-perturbative corrections depend on the chosen weight function ω.

For the kinematic weight

$$\omega_\tau \equiv (1-x)^2(1+2x), \tag{1.2.3}$$

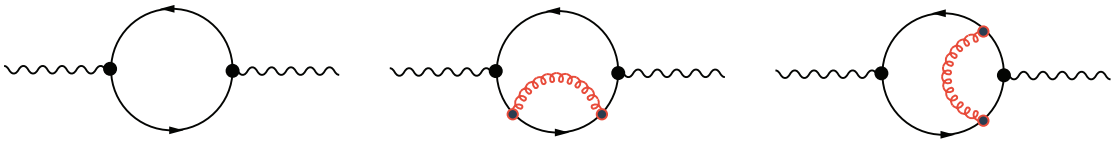

(a) (b) (c)

we have a dominant perturbative contribution of $\delta_{pt} \approx 20\%$ [**Pich2013**] and a minor, but not negligible, non-perturbative contribution of $\delta_{npt} = -0.007 \pm 0.004$ [**Braaten1991**].

We now want to derive the theoretical expressions needed to calculate both of the corrections to eq. 1.2.2 starting with the perturbative one.

1.2.1 The perturbative contribution

The perturbative contribution δ_{pt} to the inclusive tau decay ratio is given as the first term of the OPE. Currently the perturbative expansion has been calculated to fourth order $\mathcal{O}(\alpha_s^4)$. Due to their role as dominant corrections their uncertainties from unknown higher-order corrections dominate the final error of the determination of the strong coupling [**Pich2016**].

We will treat the correlator in the chiral limit, in which the scalar and pseudoscalar contribution of the two-point function vanish and the axial and vectorial contributions are equal. As a result we can focus ourselves of the vector correlation function two-point function $\Pi_V(s)$, which can be expanded as a sum over different orders of α [**Beneke2008**]:

$$\Pi_V^{(1+0)}(s) = -\frac{N_c}{12\pi^2} \sum_{n=0}^{\infty} a_\mu^n \sum_{k=0}^{n+1} c_{n,k} L^k \quad \text{with} \quad L \equiv \ln \frac{-s}{\mu^2}. \tag{1.2.4}$$

The coefficient $c_{n,k}$ up to two-loop order can be obtained by Feynman diagram calculations. With the diagrams of section 1.2.1 can calculate the zero-loop result of the correlator [**Jamin2006**]

$$\Pi_{\mu\nu}^B(q^2)\Big|^{1-\text{loop}} = \frac{N_c}{12\pi^2}\left(\frac{1}{\hat{\epsilon}} - \log\frac{(-q^2 - i0)}{\mu^2} + \frac{5}{3} + \mathcal{O}(\epsilon)\right), \tag{1.2.5}$$

where $\Pi_{\mu\nu}^B(q^2)$ is the bare two-point function and is not renormalised[1] This result can then be used to extract the first two coefficients of the correlator

[1] The term $1/\hat{\epsilon}$, which is of order zero in α_s, will be cancelled by renormalisation.

expansion given in eq. 1.2.4

$$c_{00} = -\frac{5}{3} \qquad \text{and} \qquad c_{01} = 1. \tag{1.2.6}$$

The second loop can also be calculated by diagram techniques resulting in [**Boito2011**]

$$\Pi_V^{(1+0)}(s)\Big|^{2-\text{loop}} = -\frac{N_c}{12\pi^2}a_\mu \log(\frac{-s}{\mu^2}) + \cdots \tag{1.2.7}$$

yielding $c_{11} = 1$.

Beginning from three loop diagrams the algebra becomes exhausting and one has to use dedicated algorithms to compute the higher loops. The third loop calculations have been done in the late seventies by [**Chetyrkin1979**, **Dine1979**, **Celmaster1979**]. The four loop evaluation have been completed a little more than ten years later by [**Gorishnii1990**, **Surguladze1990**]. The highest loop published, that amounts to α_s^4, was published in 2008 [**Baikov2008**] almost 20 years later.

Fixing the number of colors to $N_c = 3$ the missing coefficients up to order four in α_s read:

$$\begin{aligned} c_{2,1} &= \frac{365}{24} - 11\zeta_3 - \left(\frac{11}{12} - \frac{2}{3}\zeta_3\right) N_f \\ c_{3,1} &= \frac{87029}{288} - \frac{1103}{4}\zeta_3 + \frac{275}{6}\zeta_5 \\ &\quad - \left(\frac{7847}{216} - \frac{262}{9}\zeta_3 + \frac{25}{9}\zeta_5\right) N_f + \left(\frac{151}{162} - \frac{19}{27}\zeta_3\right) N_f^2 \\ c_{4,1} &= \frac{78631453}{20736} - \frac{1704247}{432}\zeta_3 + \frac{4185}{8}\zeta_3^2 + \frac{34165}{96}\zeta_5 - \frac{1995}{16}\zeta_7, \end{aligned} \tag{1.2.8}$$

where used the flavor number $N_f = 3$ for the last line.

The 6-loop calculation has until today not been achieved, but Beneke and Jamin [**Beneke2008**] used and educated guess to estimate the coefficient

$$c_{5,1} \approx 283 \pm 283. \tag{1.2.9}$$

In stating the coefficients $c_{n,k}$ of the correlator expansion we have restricted ourselves to k-indices equal to one. This is due to the RGE, which relates coefficients with k different than one to the already stated coefficients $c_{n,1}$. To relate the coefficients we have to make use of the RGE. Consequently the correlator $\Pi_V^{T+L}(s)$ needs to be a physical quantity, which we can be achieved

with the previously defined Adler function (eq. 1.1.8). The correct expression for the correlator expansion in eq. 1.2.4 is then given by

$$D_V^{(1+0)} = -s\frac{d\Pi_V^{(1+0)}(s)}{ds} = \frac{N_c}{12\pi^2}\sum_{n=0}^{\infty} a_\mu^n \sum_{k=1}^{n+1} k c_{n,k} L^{k-1}, \tag{1.2.10}$$

where we used $dL^k/ds = k\ln(-s/\mu^2)^{k-1}(-1/\mu^2)$. Applying the RGE (**??**) to the scale-invariant Adler function yields

$$-\mu\frac{d}{d\mu}D_V^{(1+0)} = -\mu\frac{d}{d\mu}\left(\tfrac{\partial}{\partial L}\,dL + \tfrac{\partial}{\partial a_s}\,da_s\right)D_V^{1+0} = \left(2\tfrac{\partial}{\partial L} + \beta\tfrac{\partial}{\partial a_s}\right)D_V^{1+0} = 0, \tag{1.2.11}$$

where we made use of the β function, which is defined in **??**, and of the expression $dL/d\mu = -2/\mu$.

The relation between the correlator expansion coefficients can then be taken by calculating the Adler function for a desired order and plugging it into the RGE. For example the Adler function to the second order in α_s

$$D(s) = \frac{N_c}{12\pi^2}\left[c_{01} + a_\mu(c_{11} + 2c_{12}L) + a_\mu^2(c_{21} + 2c_{22}L + 3c_{23}L^2)\right], \tag{1.2.12}$$

can be inserted into RGEAdler

$$4a_\mu c_{12} + 2a_\mu^2(2c_{22} + 6c_{23}L) + \beta_1 a_\mu^2(c_{11} + 2c_{12}L) + \mathcal{O}(a_\mu^3) = 0 \tag{1.2.13}$$

to compare the coefficients order by order in α_s. At order α_μ only the c_{12} term is present and has consequently to be zero. For $\mathcal{O}(a_\mu^2 L)$ only c_{23} exists as $c_{12} = 0$ and thus also has to vanish. Finally at $\mathcal{O}(a)$ we can relate c_{22} with c_{11} resulting in:

$$c_{12} = 0, \quad c_{22} = \frac{\beta_1 c_{11}}{4} \quad \text{and} \quad c_{23} = 0. \tag{1.2.14}$$

Implementing the newly obtained Adler coefficients we can write out the Adler function to the first order:

$$D(s) = \frac{N_c}{12\pi^2}\left[c_{01} + c_{11}a_\mu\left(c_{21} - \frac{1}{2}\beta_1 c_{11}L\right)a_\mu^2\right] + \mathcal{O}(a_\mu^3). \tag{1.2.15}$$

continue here We have used the RGE to relate Adler-function coefficients and thus reduce its numbers. But as we will see in the following section the RGE gives us two different choices in the order of the computation of the perturbative contribution to the inclusive tau decay ratio.

Renormalization group summation

By making use of the RGE we have to decide about the order of mathematical operations we perform. As the perturbative contribution δ_{pt} is independent on the scale μ we are confronted with two choices *fixed-order perturbation theory* (FOPT) or *contour-improved perturbation theory* (CIPT). Each of them yields a different result, which is the main source of error in extracting the strong coupling from tau decays.

We can write the perturbative contribution δ_{pt} of R_τ (eq. 1.2.2) in the chiral limit, such that the longitudinal contribution $D^{(0)}$, in eq. 1.1.14 vanishes. Thus inserting the expansion of $D_V^{(1+0)}$ into the hadronic tau decay width eq. 1.1.14 yields

$$\delta_{pt} = \sum_{n=1}^{\infty} a_\mu^n \sum_{k=1}^{n} k c_{n,k} \frac{1}{2\pi i} \oint_{|x|=1} \frac{dx}{x} (1-x)^3 (1+x) \log\left(\frac{-m_\tau^2 x}{\mu^2}\right)^{k-1}. \tag{1.2.16}$$

Keep in mind that the contributions from the vector and axial-vector correlator are identical in the massless case:

$$D^{(1+0)} = D_V^{(1+0)} + D_A^{(1+0)} = 2D_V^{(1+0)}. \tag{1.2.17}$$

To continue evaluating the perturbative part we can now either follow the description of FOPT or CIPT. We will now present both.

In FOPT we fix the scale at the tau mass ($\mu^2 = m_\tau^2$), which leaves us with the integration over the logarithm, as seen in

$$\delta_{FO}^{(0)} = \sum_{n=1}^{\infty} a(m_\tau^2)^n \sum_{k=1}^{n} k c_{n,k} J_{k-1} \tag{1.2.18}$$

where the contour integrals J_l are defined by

$$J_l \equiv \frac{1}{2\pi i} \oint_{|x|=1} \frac{dx}{x} (1-x)^3 (1+x) \log^l(-x). \tag{1.2.19}$$

The integrals J_l up to order α_s^4 are given by [**Beneke2008**]:

$$J_0 = 1, \quad J_1 = -\frac{19}{12} \quad J_2 = \frac{265}{72} - \frac{1}{3}\pi^2, \quad J_3 = -\frac{3355}{288} + \frac{19}{12}\pi^2. \tag{1.2.20}$$

Using FOPT the strong coupling $a(\mu)$ is fixed at the tau mass scale $a(m_\tau^2)$ and can be taken out of the closed-contour integral. Thus we solely have to integrate over the logarithms $\log(x)$.

Using CIPT we can sum the logarithms by setting the scale to $\mu^2 = -m_\tau^2 x$ in eq. 1.2.16, resulting in:

$$\delta_{CI}^{(0)} = \sum_{n=1}^{\infty} c_{n,1} J_n^a(m_\tau^2), \tag{1.2.21}$$

where the contour integrals J_l are defined by

$$J_n^a(m_\tau^2) \equiv \frac{1}{2\pi i} \oint_{|x|=1} \frac{dx}{x} (1-x)^3 (1+x) a^n(-m_\tau^2 x). \tag{1.2.22}$$

Note that all logarithms vanish, except the ones with index $k = 1$:

$$\log(1)^{k-1} = \begin{cases} 1 & \text{if } k = 1, \\ 0 & k \neq 1 \end{cases} \tag{1.2.23}$$

which selects the Adler function coefficients $c_{n,1}$. Handling the logarithms left us with the integration of $\alpha_s(-m_\tau^2 x)$ over the closed-contour $\oint_{|x|=1}$, which now depends on the integration variable x.

In general we have to decide if we want to perform a contour integration with a constant coupling constant and variable logarithms (FOPT) or "constant logarithms" and a running coupling (CIPT). To emphasize the differences in both approaches we can calculate the perturbative contribution $\delta^{(0)}$ to R_τ for the two different prescriptions yielding [**Beneke2008**]

$$\begin{aligned} & \alpha_s^2 \quad \alpha_s^2 \quad \alpha_s^3 \quad \alpha_s^4 \quad \alpha_s^5 \\ \delta_{FO}^{(0)} &= 0.1082 + 0.0609 + 0.0334 + 0.0174(+0.0088) = 0.2200(0.2288) && (1.2.24) \\ \delta_{CI}^{(0)} &= 0.1479 + 0.0297 + 0.0122 + 0.0086(+0.0038) = 0.1984(0.2021). && (1.2.25) \end{aligned}$$

The series indicate, that CIPT converges faster and that both series approach a different value. This discrepancy represents currently the biggest theoretical uncertainty while extracting the strong coupling.

As today we do not know if FOPT or CIPT is the correct approach of measuring the strong coupling. Therefore there are currently three ways of stating results: Quoting the average of both results, quoting the CIPT result or quoting the FOPT result. We follow the approach of Beneke and Jamin [**Beneke2008**] who prefere FOPT, but also state their results in CIPT.

1.2.2 The Non-Perturbative OPE Contribution

The perturbative contribution to the sum rule is the dominant one. The contribution of the NPT part can be quoted as

$$\delta_{NP} = 0,007 \pm 0.004 \qquad [\textbf{Braaten1991}], \tag{1.2.26}$$

which is small, but not negligible. The NP OPE contributions are commonly categorised by even, increasing dimensions. Contributions of dimension larger than eight are normally neglected, due to the increasing suppression by factors of $1/m_\tau^{2D}$, where D stands for the corresponding dimension.

The dimension two contributions are proportional to the quark masses. As we are working in the chiral limit we will neglect them.

1.2.3 Dimension four

The next apparent OPE contribution is of dimension four. Here we have to take into account the terms with masses to the fourth power m^4, the quark condensate multiplied by a mass $m\langle\overline{q}\,q\rangle$ and the gluon condensate $\langle GG\rangle$. The resulting expression can be taken from the appendix of **[Pich1999]**, yielding:

$$D_{ij}^{(1+0)}(s)\Big|_{D=4} = \frac{1}{s^2}\sum_n \Omega^{(1+0)}(s/\mu^2)a^n, \tag{1.2.27}$$

where

$$\begin{aligned}\Omega_n^{(1+0)}(s/\mu^2) \;=\; & \frac{1}{6}\langle aGG\rangle p_n^{(1+0)}(s/\mu^2) + \sum_k m_k\langle\overline{q}_k q_k\rangle r_n^{(1+0)}(s/\mu^2) \\ & + 2\langle m_i\overline{q}_i q_i + m_j\overline{q}_j q_j\rangle q_n^{(1+0)}(s/\mu^2) \pm \frac{8}{3}\langle m_j\overline{q}_i q_i + m_i\overline{q}_j q_j\rangle t_n^{(1+0)} \\ & - \frac{3}{\pi^2}(m_i^4 + m_j^4)h_n^{(1+0)}(s/\mu^2) \mp \frac{5}{\pi^2}m_i m_j(m_i^2 + m_j^2)k_n^{(1+0)}(s/\mu^2) \\ & + \frac{3}{\pi^2}m_i^2 m_j^2 g_n^{(1+0)}(s/\mu^2) + \sum_k m_k^4 j_n^{(1+0)}(s/\mu^2) + 2\sum_{k\neq l} m_k^2 m_l^2 u_n^{(1+0)}(s/\mu^2)\end{aligned} \tag{1.2.28}$$

The perturbative expansion coefficients are known to $\mathcal{O}(a^2)$ for the condensate contributions,

$$\begin{array}{lll} p_0^{(1+0)} = 0, & p_1^{(1+0)} = 1, & p_2^{(1+0)} = \frac{7}{6}, \\ r_0^{(1+0)} = 0, & r_1^{(1+0)} = 0, & r_2^{(1+0)} = -\frac{5}{3} + \frac{8}{3}\zeta_3 - \frac{2}{3}\log(s/\mu^2), \\ q_0^{(1+0)} = 1, & q_1^{(1+0)} = -1, & q_2^{(1+0)} = -\frac{131}{24} + \frac{9}{4}\log(s/\mu^2) \\ t_0^{(1+0)} = 0 & t_1^{(1+0)} = 1, & t_2^{(1+0)} = \frac{17}{2} + \frac{9}{2}\log(s/\mu^2). \end{array} \tag{1.2.29}$$

while the m^4 terms have been only computed to $\mathcal{O}(a)$

$$\begin{aligned}
h_0^{(1+0)} &= 1 - 1/2\log(s/\mu^2), & h_1^{(1+0)} &= \tfrac{25}{4} - 2\zeta_3 - \tfrac{25}{6}\log(s/\mu^2) - 2\log(s/\mu^2)^2,\\
k_0^{(1+0)} &= 0, & k_1^{(1+0)} &= 1 - \tfrac{2}{5}\log(s/\mu^2),\\
g_0^{(1+0)} &= 1, & g_1^{(1+0)} &= \tfrac{94}{9} - \tfrac{4}{3}\zeta_3 - 4\log(s/\mu^2),\\
j_0^{(1+0)} &= 0, & j_1^{(1+0)} &= 0,\\
u_0^{(1+0)} &= 0, & u_2^{(1+0)} &= 0.
\end{aligned} \tag{1.2.30}$$

1.2.4 Dimension six and eight

Our application of dimension six contributions is founded in [**Braaten1991**] and has previously been calculated beyond leading order by [**Lanin1986**]. The operators appearing are the masses to the power six m^6, the four-quark condensates $\langle \overline{q}\, q \overline{q}\, q \rangle$, the three-gluon condensates $\langle g^3 G^3 \rangle$ and lower dimensional condensates multiplies by the corresponding masses, such that in total the mass dimension of the operator will be six. As there are too many parameters to be fitted with experimental data we have to omit some of them, starting with the three-gluon condensate, which does not contribute at leading order. The four-quark condensates known up to $\mathcal{O}(a^2)$, but we will make use of the *vacuum saturation approach* [**Beneke2008**, **Braaten1991**, **Shifman1978**] to express them in quark, anti-quark condensates $\langle q\overline{q} \rangle$. In our work we take the simplest approach possible: Introducing an effective dimension six coefficient $\rho_{V/A}^{(6)}$ divided by the appropriate power in s

$$D_{ij,V/A}^{(1+0)}\Big|_{D=6} = 0.03\frac{\rho_{V/A}^{(6)}}{s^3} \tag{1.2.31}$$

As for the dimension eight contribution the situation is not better than the dimension six one we keep the simplest approach, leading to

$$D_{ij,V/A}^{(1+0)}\Big|_{D=8} = 0.04\frac{\rho_{V/A}^{(8)}}{s^4}. \tag{1.2.32}$$

1.3 Duality Violations

As seen in **??** we have to assume quark-hadron duality for the QCDSR to work. Unfortunately duality cannot always be taken for granted and the existence

of *duality violations* (DV) is a well known [**Cata2008**, **Cata2009**]. As we will see in the following section, the experimental measured total tau decay ratio has a exponential decreasing, sinusoidal contributions, that cannot be reproduced by the OPE solely. Consequently for the cases with apparent DV we also have to take into account DV corrections and adapt eq. 1.2.2

$$R^{\omega}_{\tau,V/A} = \frac{N_c}{2} S_{EW} |V_{ud}|^2 \left(1 + \delta^{\omega}_{pt} + \delta^{\omega}_{npt} + \delta^{\omega}_{dv}\right). \tag{1.3.1}$$

The DV correction has been modelled by a series of papers [**Boito2011a**, **Boito2012**, **Boito2014**] with the following ansatz

$$\rho^{DV}_{V/A}(s) = e^{-(\delta_{V/A} + \gamma_{V/A} s)} \sin(\alpha_{V/A} + \beta_{V/A} s), \tag{1.3.2}$$

to parametrise the DV contributions. The DV would then appear as an additional term in the inclusive tau decay ratio

$$R_{\tau,V/A} = -\pi i \oint_{|s|=m_\tau^2} \frac{dx}{x}(1-x)^3 \left[3(1+x)D^{(1+0)}(m_\tau^2 x) + 4D^{(0)}(m_\tau^2 x)\right] + \mathcal{D}_{V/A}(m_\tau^2), \tag{1.3.3}$$

where the DV would be given as

$$\mathcal{D}_{\omega}(m_\tau^2) = -12\pi^2 \int_{m_\tau^2}^{\infty} \frac{ds}{m_\tau^2} \omega(s) \rho_{V/A}. \tag{1.3.4}$$

1.3.1 Pinched weights to avoid DVs

We are free to multiply **??** by an analytic weight function $\omega(s)$

$$\int_0^{m_\tau} \omega(s)\Pi(s)\, ds = \frac{i}{2} \oint_{s=m_\tau} \omega(s)\Pi(s)\, ds. \tag{1.3.5}$$

We can use this technique to suppress contributions for the two-point function close to the positive real axis by implementing so called pinched weights of the form

$$\omega(s) = \left(1 - \frac{s}{m_\tau^2}\right)^k, \tag{1.3.6}$$

where k is the degree of the pinched weight. The higher the degree the farther we operate from the critical positive real axis (see. **??**), which suppresses the effects of duality violations. This pinching of second degree appears quite naturally. If we regard the include $\tau - decay$ ratio eq. 1.1.3, we note that for the

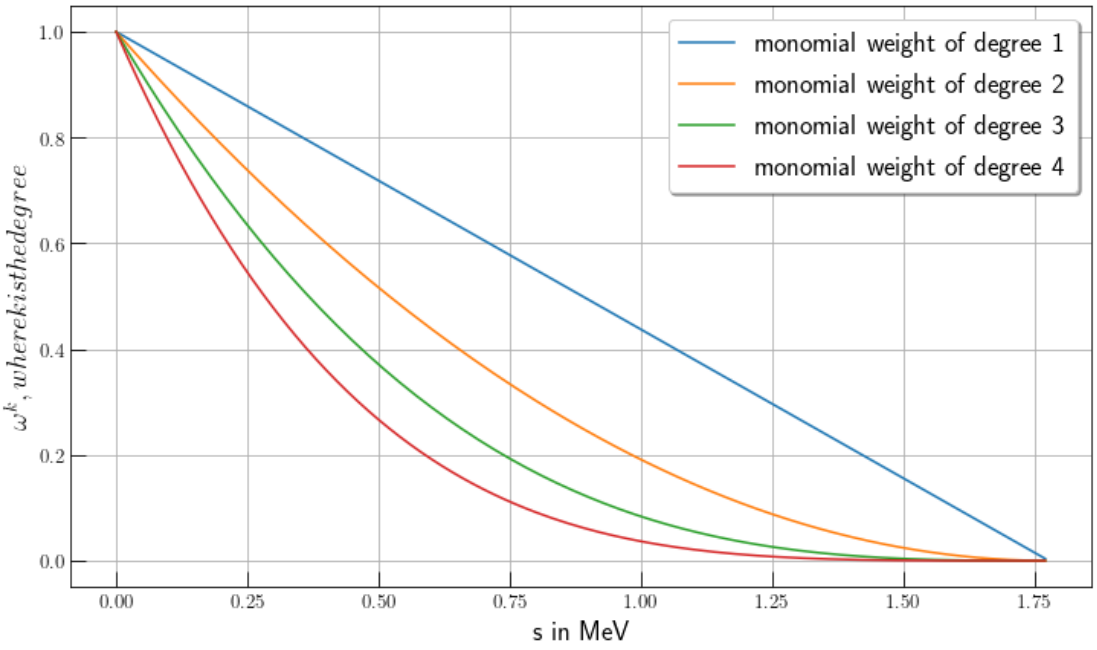

Figure 1.1: Monomial weights $(1 - s/m_\tau^2)^k$ for degrees $1 \to 4$. We can see that weights of higher pinching decrease faster, which comes in handy if we want to suppress duality violations.

transversal component we already have a double pinched weight, the *kinematic weight*

$$\omega_\tau(s) = \left(1 - \frac{s}{m_\tau^2}\right)^2 \left(1 + 2\frac{s}{m_\tau^2}\right). \tag{1.3.7}$$

In general it is said that a double pinched weight is sufficient to neglect effects caused by duality violation.

1.4 Experiment

The tau decay data we use to perform our QCD analysis is from the ALEPH experiment. The ALEPH experiment was located at the *large-electron-positron* (LEP) collider at *European Organisation for Nuclear Research* (CERN) in Geneva. LEP started producing particles in 1989 and was replaced in the late 90s by the *large-hadron-collider* (LHC), which makes use of the same tunnel of 27 km circumference. The data produced within the experiment is still maintained by former ALEPH group members under led by M. Davier, which have performed regular updates on the data-sets [**Davier2013**, **Davier2008**, **Aleph2005**].

The measured spectral functions for the ALEPH data are defined in [**Davier2007**] and given for the transverse and longitudinal components separately

$$\begin{aligned}\rho^{(1)}_{V/A}(s) = &\frac{m_\tau^2}{12|V_{ud}|^2 S_{EW}} \frac{\mathcal{B}(\tau^- \to V^-/A^- \nu_\tau)}{\mathcal{B}(\tau^- \to e^- \overline{\nu}_e \nu_\tau)} \\ &\times \frac{dN_{V/A}}{N_{V/A}\, ds} \left[\left(1 - \frac{s}{m_\tau^2}\right)^2 \left(1 + \frac{2s}{m_\tau^2}\right)\right]^{-1} \\ \rho^{(0)}_{A}(s) = &\frac{m_\tau^2}{12|V_{ud}|^2 S_{EW}} \frac{\mathcal{B}(\tau^- \to \pi^-(K^-)\nu_\tau)}{\mathcal{B}(\tau^- \to e^- \overline{\nu}_e \nu_\tau)} \times \frac{dN_A}{N_A\, ds} \left(1 - \frac{s}{m_\tau^2}\right)^{-2}.\end{aligned} \tag{1.4.1}$$

$$\mathcal{B}_e = \ldots \tag{1.4.2}$$

$$R_{\tau,V/A} = \frac{B_{V/A,\tau}}{B_e} \tag{1.4.3}$$

The data relies on a separation into vector and axial-vector channels. In the case of the pions this can be achieved via counting. The vector channel is characterised by a negative parity, whereas the axial-vector channel has positive parity. A quark has by definition positive parity, thus an anti-quark has a negative parity. A meson, like the pion particle, is a composite particle consisting of an quark an anti-quark. Consequently a single pion carries negative parity, an even number of Pions carries positive parity and an odd number of Pions carries negative parity:

$$n \times \pi = \begin{cases} \text{vector} & \text{if } n \text{ is even,} \\ \text{axial-vector} & \text{otherwise} \end{cases}. \tag{1.4.4}$$

The contributions to the spectral function for the vector, axial-vector and V+A channel can be seen in fig. 1.2. The dominant modes in the vector case are [**Davier2006**] $\tau^- \to \pi^-\pi^0\nu_\tau$ and the $\tau^- \to \pi^-\pi^-\pi^+\pi^0\nu_\tau$. The first of these is produced by the $\rho(770)$ meson, which in contrary to the pions carries angular momentum of one, which is also clearly visible as peak around 770 GeV in fig. 1.2a. The dominant modes in the axial-vector case are $\tau^- \to \pi^-\nu_\tau$, $\tau^- \to \pi^-\pi^0\pi^0\nu_\tau$ and $\tau^- \to \pi^-\pi^-\pi^+\nu_\tau$. Here the three pion final states stem from the a_1^--meson, which is also clearly visible as a peak in fig. 1.2b.

We furthermore added the perturbative result for a fixed $\alpha_s(m_\tau) = 0.329$ using FOPT in fig. 1.2c. Here we can see, that the perturbative result (the blue line)

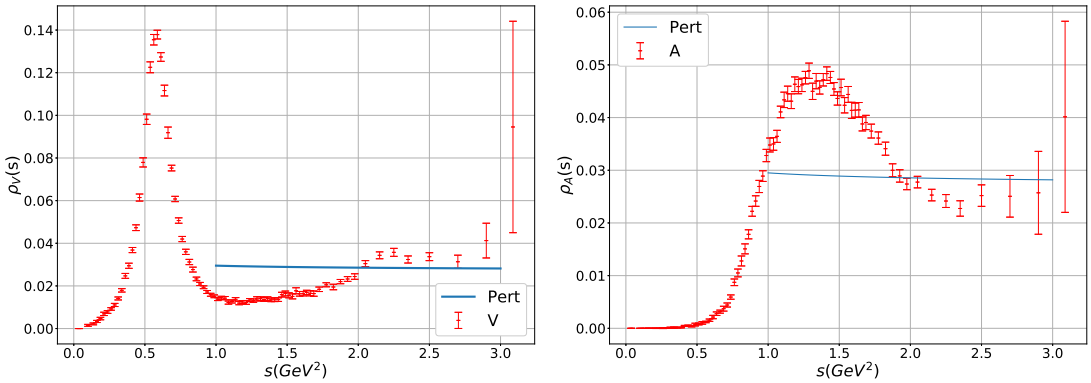

(a) Vector

(b) Axial-Vector

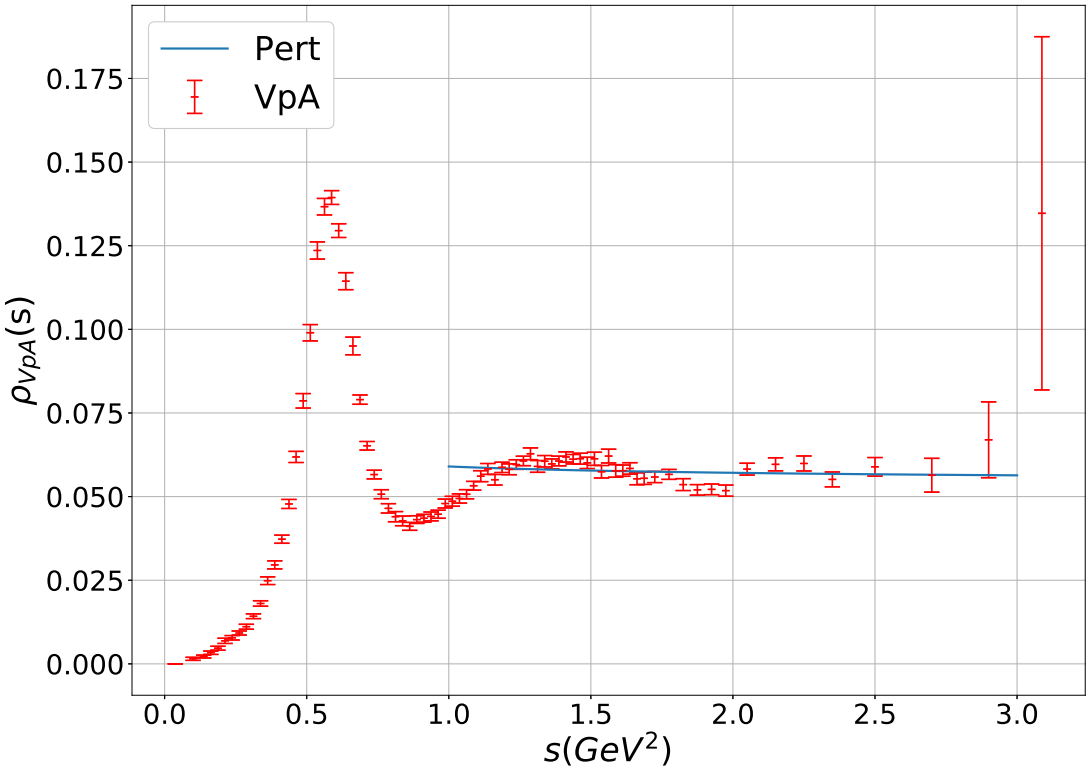

(c) Vector plus Axial-Vector

Figure 1.2: Visualisation of the vector, axial-vector and V+A spectral function given by the ALEPH data [**Davier2013**] in red with errors. We also plotted the FOPT theoretical calculation up to third order in α_s, for a fixed $\alpha_s(\tau) = 0.329$ in blue. Note that the perturbative contribution can only limited represent the experimental data. It does not reproduce the sinusoidal form.

is an almost straight line and cannot reproduce the sinusoidal graph, given by the ALEPH data. This is especially the case for the V and A channel and is seen as an indicator for DV. Even including NP, higher dimensions of the OPE is not reproducing the wavy structure. In the case of V+A, we have an higher agreement between our perturbative graph and the data. In general we believe that DV are sufficiently suppressed in the case of V+A and will argument in favour of this statement in the following chapter. This is only the case for energies larger than 1.5 GeV, as the ρ resonance of the V channel is impossible to be represented by perturbative tools. For lower energies DV become to important to be neglected.

1.4.1 Total decay ratio from experimental data

The data has been last revised in 2014 [**Davier2014**] and is publicly available [**AlephData**]. It consists of the mass squared bin center *sbin*, the bin size *dsbin*, the normalised invariant mass squared distribution *sfm2*, the total errors *derr* and their correlations *corerr*. To make the data comparable to our theoretical calculations we have to give the normalised invariant mass squared distribution *sfm2* in form of the total decay ratio R_τ. The data is given as the normalised invariant mass squared distribution $(dN_i/ds)/N_i$ scaled by a factor 100 and further normalised to the corresponding branching ratio $i \in \{V,A,VpA\}$. Thus we can connect the branching ratio of the i-channel to *sfm2* as follows

$$\mathcal{B}_{V/A} \equiv \int_0^{s_\tau} ds \frac{sfm2_{V/A}(s)}{100} \equiv \int_0^{s_\tau} ds \mathcal{B}_{V/A} \left(\frac{dN_{V/A}}{N_{V/A}\, ds} \right) \tag{1.4.5}$$

where we defined $s_\tau \equiv m_\tau^2$. The total decay ratio R_τ is defined as the decay width of taus decaying into hadrons over taus decaying into electrons and can be expressed via the corresponding branching ratios, which then can be connected to the invariant mass squared distribution sfm2

$$R_{\tau,V/A} = \frac{\mathcal{B}_{V/A}}{\mathcal{B}_|} = \int_0^{s_\tau} ds \frac{sfm2_{V/A}(s)}{100 \mathcal{B}_e}. \tag{1.4.6}$$

Theoretically the decay ratio is given in **??**. If we neglect the longitudinal contribution $\mathrm{Im}\,\Pi^{(0)}(s)$ and remember the definition of the spectral function (**??**) and the kinematic weight (eq. 1.3.7), we can write the decay ratio as

$$R_{\tau,i} = \int_0^{s_\tau} \frac{difs}{s_\tau} \omega_\tau(s) \rho(s) \tag{1.4.7}$$

and thus relate the spectral function to the experimental data

$$\Rightarrow \rho(s) = \frac{s_\tau}{12\pi^2 100\mathcal{B}_e}\frac{\text{sfm2}}{\omega_\tau}. \tag{1.4.8}$$

To fit the experimental data we define a so-called *spectral function moment* (or *moment*)

$$I_i^{\text{exp},\omega} \equiv \int_0^{s_0}\frac{ds}{s_0}\omega\left(\frac{s}{s_0}\right)\rho(s), \tag{1.4.9}$$

which will be used in our χ^2 fits, explained in the upcoming section. The data is given for discrete bins so we have to express the integral of the spectral function moment as sum over those bins. The final expression we use to fit parameters to the experimental data is then given by

$$I^{\omega}_{\text{exp},V/A}(s_0) = \frac{s_\tau}{100\mathcal{B}_e s_0}\sum_{i=1}^{N(s_0)}\frac{\omega\left(\frac{s_i}{s_0}\right)}{\omega_\tau\left(\frac{s_i}{s_\tau}\right)}\,\text{sfm2}_{V/A}(s_i). \tag{1.4.10}$$

1.5 The Method of Least Squares

We apply *method of least squares* (LS) to fit the parameters $\vec{\alpha}$ from the experimental data. We consequently construct a χ^2-function

$$\chi^2 = \left(I_i^{\text{exp}} - I_i^{\text{th}}(\vec{\alpha})\right) C_{ij}^{\text{exp}\,-1}\left(I_j^{\text{exp}} - I_j^{\text{th}}(\vec{\alpha})\right), \tag{1.5.1}$$

where I^{exp}/ I^{th} is a vector of experimental moments/ theoretical moments with the same weight, but different energy cutoffs s_0, labelled by the index i. In addition C^{exp} is the covariance matrix describing the correlation of the different experimental moments $C_{ij}^{\text{exp}} = \text{cov}[I_i^{\text{exp}} I_j^{\text{exp}}]$, which is given by the ALEPH data.

In general we aim to minimise the value of χ^2, which will fix the parameter vector $\vec{\alpha}$. The properties of the χ^2-function are well known and the best fits are characterised through $\chi^2/\text{dof} \approx 1$, where the DOF of the fit can be calculated through

$$\text{DOF} = \text{experimental moments} - \text{parameters}. \tag{1.5.2}$$

E.g. if we want to fit α_s and the dimension four Wilson coefficient C_4 we get $7 - 2 = 5$ DOF.

The parameter vector $\vec{\alpha}$ includes the strong coupling α_s, but also the included OPE Wilson coefficient. Consequently we should have at least as many, if not more moments as parameters we want to fit. As the moments for different s_0 are highly correlated we are limited to fit a set of only a few parameters.

It is also possible to increase the number of moments used by using multiple weights ω. Unfortunately using different weights leads to highly correlated moments, which leads to numerical complications by inverting the covariance matrix in eq. 1.5.1. To handle the high correlations we have to redefine our fit quality.

1.5.1 Block Diagonal "Fit-Quality"

Following [**Boito2014**] we can redefine LS to

$$Q^2 = \sum_{\omega} \sum_{s_0^i, s_0^j} \left(I_\omega^{exp}(s_0^i) - I_\omega^{th}(s_0^i, \vec{\alpha}) \right) \widetilde{C}^{-1}_{ij,\omega} \left(I_\omega^{exp}(s_0^j) - I_\omega^{th}(s_0^j, \vec{\alpha}) \right), \tag{1.5.3}$$

where the covariance matrix $\widetilde{C}$ is now a diagonal of the experimental covariance matrices C_ω^{exp} for each weight

$$\widetilde{C} = \begin{pmatrix} C^{exp}_{\omega=1} & 0 & \dots & 0 \\ 0 & C^{exp}_{\omega=2} & \ddots & \vdots \\ \vdots & \ddots & \ddots & 0 \\ 0 & \dots & 0 & C^{exp}_{\omega=n} \end{pmatrix}. \tag{1.5.4}$$

As a result we are still able to invert the newly defined covariance matrix $\widetilde{C}$, but minimisation routines like CERN MINUIT are now able to calculate the proper errors for the parameters we want to extract. We have to perform our own error propagation to obtain meaningful errors for the parameters.

Error Propagation

The error propagation has been derived in [**Boito2011a**, **Boito2011**] and is given as

$$\langle \delta\alpha_k \alpha_l \rangle = A^{-1}_{km} A^{-1}_{ln} \frac{\partial I_i^{th}(\vec{\alpha})}{\partial \alpha_m} \frac{\partial I_r^{th}(\vec{\alpha})}{\partial \alpha_n} \widetilde{C}^{-1}_{ij} \widetilde{C}^{-1}_{ij} \langle \delta I_k^{exp} \delta I_l^{exp} \rangle, \tag{1.5.5}$$

where

$$A_{kl} = \frac{\partial I^{th}(\vec{\alpha})}{\partial \alpha_k} C^{-1}_{ij} \frac{I^{th}_j(\vec{\alpha})}{\alpha_l}. \tag{1.5.6}$$